Aircraft Normal Modes…Friend or Foe? An Airbus Answer

Mercedes Oliver Herrero
Airbus Defence and Space / TEAGD Aeroelasticity and Structural Dynamics
John Lennon s/n, 28906 Getafe, Spain
mercedes.oliver-herrero@airbus.com

Félix Arévalo Lozano
Airbus Defence and Space / TEAGD Aeroelasticity and Structural Dynamics

Héctor Climent Máñez
Airbus Defence and Space / TEAGD Aeroelasticity and Structural Dynamics

ABSTRACT

Dynamic loads and Aeroelasticity have played a relevant role in the history of aviation and continue being two of the most important aspects in the aircrafts design and certification process. Dynamic Loads (Gust/Turbulence, Dynamic Landing, Taxiing, etc.) are often amongst the sizing critical load cases in many aircraft components, while Aeroelasticity determines not only the lifting and control surfaces design but also the maintainability requirements after the aircraft entry into service. The classical approach to solve response-type (Loads) or instability (Aeroelasticity) problems relies on considering that the aircraft structure flexible deformation can be written as a combination of the zero-damped structure normal modes. This paper aims to show the normal modes relevance in the solution of Structural Dynamics and Aeroelastic problems in general and the Airbus civil and military aircrafts specificities when analysed from a normal modes point of view.

KEYWORDS: *Structural Dynamics, Aeroelasticity, Normal modes, Dynamic Loads, Flutter*

NOMENCLATURE

A/C	Aircraft
CPU	Central Processing Unit
DTG	Discrete Tuned Gust
EMS	Engine Mounting System
FCL	Flight Control Laws
FEM	Finite Element Method
FVT	Flight Vibration Test
GVT	Ground Vibration Test
HTP	Horizontal Tailplane
L/H	Left-hand
LG	Landing Gear
M&L	Medium & Light
MLG	Main Landing Gear
MRTT	Multi Role Tanker Transport
MTOW	Maximum Take-off Weight
NLG	Nose Landing Gear
OWE	Operational Weight Empty
PSD	Power Spectral Density
R/H	Right-hand
RMS	Root mean square
SD&A	Structural Dynamics and Aeroelasticity
VTP	Vertical Tailplane

1 INTRODUCTION

The dynamic loads and aeroelasticity analyses performed for the aircraft feasibility, design, checkstress and certification phases are based on aircraft structure dynamic equations. The dynamic equations of a system can be stated in direct form, using all the degrees of freedom of the system, or in modal approach, which is based on using information of the system response in a free vibration condition. The free vibration condition assumes that the structure is not subjected to any external excitation, the structural damping is negligible, and therefore its motion occurs only from the initial conditions of displacement and velocity. This condition is relevant because the analysis of the structure response in free motion provides substantive information regarding the dynamic properties of the structure. These properties are the natural frequencies and the corresponding vibration mode shapes, what we call the structure normal modes.

The use of normal modes base for the structure displacement linear decomposition shows to be the most accurate (compared with other approximate methods such as Rayleigh-Ritz).

On the other hand, the nature of structures normal modes make them more than a mathematical stratagem used in dynamic loads and aeroelasticity analyses: The structure displacement when harmonically excited in one of its natural resonances (a normal mode frequency), other that damp, tends to amplify. Therefore the structure deformation shape will mainly be determined by the excitation normal modes contribution.

Understanding the aircraft normal modes is, therefore, fundamental to identify the root causes of a certain dynamic response or stability phenomenon. The normal modes frequency and shape are determined by the stiffness and inertia distributions, which, in turn, are directly correlated with the aircraft configuration (e.g. low, mid, or high wing), size, design weights, and payload/fuel distribution, or the control surfaces actuators' stiffness.

2 STRUCTURAL DYNAMICS AND AEROELASTICITY IN THE A/C DESIGN AND CERTIFICATION PROCESS

2.1 Structural Dynamics and Aeroelasticity History

Throughout the history of aviation and from its very beginning, Structural Dynamics and Aeroelasticity have dramatically fostered its progress and conditioned the aircrafts conception and design. The following list shows the earliest and the most relevant events, which may be considered milestones of the SD&A history:

- Divergence, *structure collapse because of high external aerodynamic loading*:
  8/12/1903 Samuel P. Langley's *Aerodrome*
  24/01/1917 Albatross DIII
  19/08/1918 Fokker D.VIII
- Control reversal, *the control surface rotation (e.g. aileron) effect is nullified by the torsion of the fixed part (wing)*:
  1940 Mitsubishi A6M "Zero"
- Flutter, *dynamic instability caused by the coalescence of normal modes*:
  1916 Handley Page 0-400 Bomber
  1917 De Havilland DH-9
  1920 Van Berkel W.B. Monoplane
  1931 Gee Bee racer
  1939 Heinkel He 177
  1943 Gloster Meteor
  1961 Convair 990
  1970's-1980's Beech Bonanza Model 35 (likely)
  1997 F117 Stealth
- Whirl Flutter, *propeller instability*:
  1959-1960 Lockheed Electra
- Aeroservoelasticity: *coupling of flexible modes with control surfaces rotation commanded by FCL*:
  A3J-1 "Vigilante"
- Dynamic response of the flexible system under external forces:
  Dynamic Landing: 1940 Consolidated B-24 Liberator
  Taxi: 1989 Fokker 100
  Gust & Turbulence:
    1963 B-52 Stratofortress
    1966 Boeing 707 at Mount Fuji
    1982/1990 de Havilland Canada DH-6 Twin-Otter
- Buffet, *dynamic response under external wake excitation*:
  1930 Junkers F.13
  1980's F18
- Ditching, *aircraft forces in a controlled landing in water*:
  1909. Antoinette IV monoplane

Figure 1: Examples of relevant aeroelastic and dynamic loads events

Some authors point that Aeroelasticity-related effects are responsible for delaying the first controlled and sustained flight, which could have been reached by Langley on December 8, 1903 if the Divergence instability had not appeared. It is somehow exaggerated, but the real fact is that the Wright brothers had success some days later (December 17, 1903) by avoiding any aeroelastic instability (basically Divergence and Flutter) and controlling the aircraft using the torsion flexibility of the wing, both aspects related to the Aeroelasticity.

Aeroelasticity plays therefore a crucial role for the successful design of any aircraft and nowadays the state of the art has allowed not only to mitigate the negative effects of the flexibility but also to take advantage of it: aeroservoelastic active control methodology ([1]), aeroelastic tailoring, usage of the wing torsion to control the aircraft (like Wright brothers!), etc.

2.2 Structural Dynamics and Aeroelasticity today

After more than one-hundred years learning from aviation operation and understanding the root causes of accidents, the airworthiness regulations have progressively evolved in order to guarantee aircrafts safety by requesting suitable analyses and tests. In this framework, SD&A plays a fundamental role during all the aircraft life, from the design phase to the entry into service and afterwards.

For current military and civil aircrafts, dynamic loads conditions are among the sizing critical load cases. Figure 2 shows Heavy Military Transport Aircraft components dimensioned by dynamic loads or flutter.

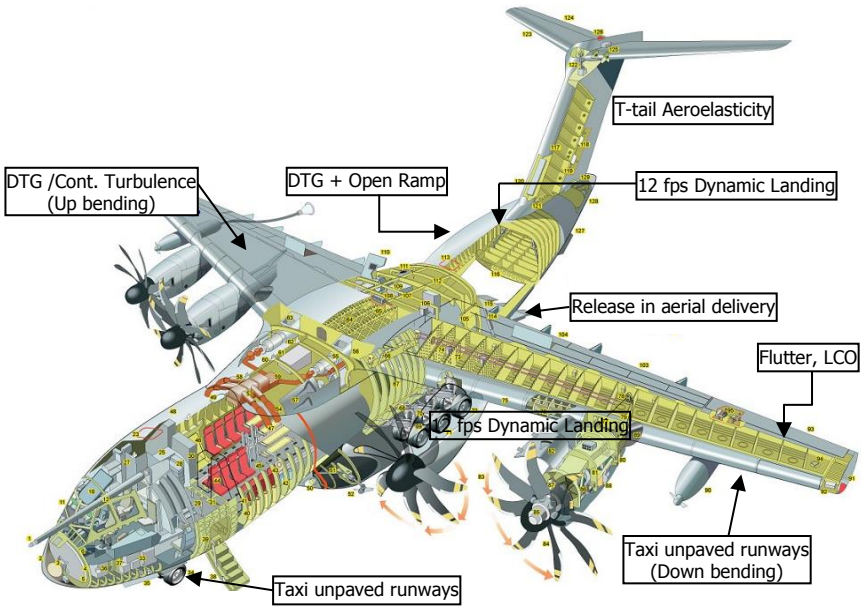

Figure 2: Military transport A/C components dimensioned by dynamic loads or flutter

On the other hand, apart from the implications of aeroelasticity in the structure or control laws design, which may impact directly in the aircraft weight or manoeuvrability, certain requirements to in-service actions, such as maintenance, repairs or painting, have the "Aeroelastics" stamp.

In the SD&A dartboard shown in Figure 3, when looking at the multiple disciplines involved, the **normal modes** are a common denominator in most of them.

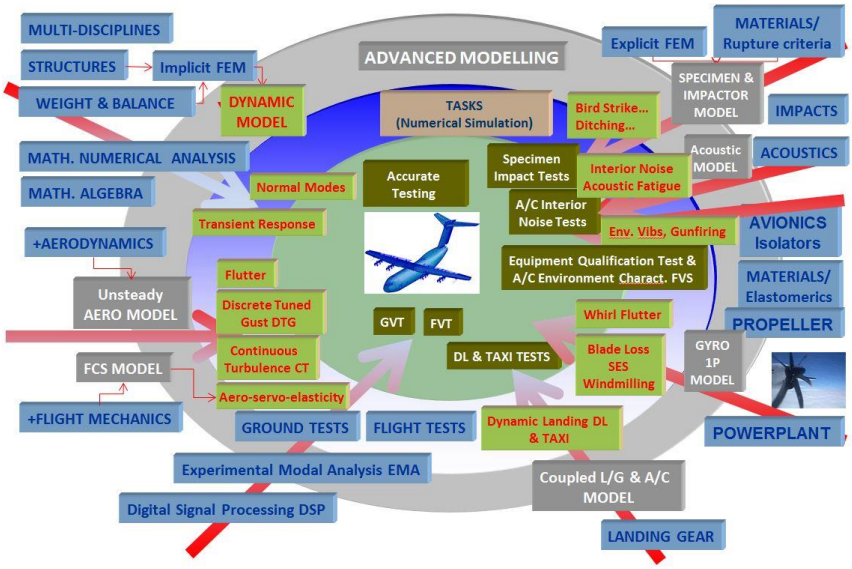

Figure 3: Structural Dynamics and Aeroelasticity dartboard

3 USE OF EIGENVALUES AND EIGENVECTORS TECHNIQUE IN SD&A PROBLEMS SOLUTION

The dynamic equations of a system are detailed into many classical books and, in particular, in aeroelastic-related references as [2] and [3]. These are written as:

$$[M] \cdot \{\ddot{x}\} + [D] \cdot \{\dot{x}\} + [K] \cdot \{x\} = \{P(t)\} \quad (2)$$

where:

$[M]$: mass matrix
$[D]$: damping matrix
$[K]$: stiffness matrix
x: displacement vector
$\dot{x}$: velocity vector
$\ddot{x}$: acceleration vector
$\{P(t)\}$: applied load as a function of time

For a free and undamped system, where $[P(t)] = [D] = [0]$, and assuming a harmonic solution,

$$[M] \cdot \{\ddot{x}\} + [K] \cdot \{x\} = \{0\} \rightarrow ([K] - \omega^2[M]) \cdot \{\phi\} = \{0\} \quad (3)$$

where:

ω: eigenfrequency or natural frequency of a free vibrating system
$\{\phi\}$: eigenvector or modal shape of a free vibrating system

Equation (3), analogue to the eigenvalue equation in linear algebra, has the non-trivial solution ($\{\phi\} \neq \{0\}$):

$$det([A] - \lambda[I]) = 0 \quad (4)$$

where

$[A] = [K] \cdot [M]^{-1}$: real square matrix
$\lambda = \omega^2$: eigenvalue
$\{x\} = \{\phi\}$: eigenvector

The size of equation (2) matrices and vectors when expressed in physical coordinates is the number of all structural degrees of freedom or, in MSC-NASTRAN terms, the g-set size G. For the current structural models size, the degrees of freedom are of the order of magnitude of 10^6, and equation (2) results to be a 10^6 size coupled equation. In spite of the High Performance Computers availability, this becomes a very costly problem, from the CPU time point of view, especially when facing hundreds of thousands calculations.

By introducing the modal transformation depicted in next equation (5), the G physical coordinates $\{x_G\}$ are substituted by the modal coordinates $\{\xi\}$ with the eigenvectors being the columns of the change of basis matrix $[\phi]$. The matrix $[\phi]$ size is G rows by N columns, being G the number of structural degrees of freedom and N the number of modes.

$$\{x_G\} = [\phi] \cdot \{\xi\} \tag{5}$$

Equation (2), then, becomes:

$$[M_G] \cdot [\phi] \cdot \{\ddot{\xi}\} + [D_G] \cdot [\phi] \cdot \{\dot{\xi}\} + [K_G] \cdot [\phi]\{\xi\} = [P(t)] \tag{6}$$

Pre-multiplying by $[\phi]^T$ and making additional assumptions regarding the damping matrix (i.e. modal damping, $[D_G]$ is substituted by $[C_G]$),

$$[m] \cdot \{\ddot{\xi}\} + [b] \cdot \{\dot{\xi}\} + [k] \cdot [\phi]\{\xi\} = [p(t)] \tag{7}$$

where

$[m] = [\phi]^T \cdot [M_G] \cdot [\phi]$; N x N real square diagonal matrix
$[b] = [\phi]^T \cdot [C_G] \cdot [\phi]$; N x N real square diagonal matrix
$[k] = [\phi]^T \cdot [K_G] \cdot [\phi]$; N x N real square diagonal matrix

Modal formulation has two advantages: equation (7) is uncoupled and its size is the number of modes, typically of the order of magnitude of 10^2. Its solution,$\{\xi(t)\}$, can be reverted to the physical coordinates $\{x_G\}$ through (5).

Examples shown in Figure 4 illustrate that few normal modes are enough to compute the aircraft response to transient excitation. It shows a Heavy Military Transport dynamic response to a discrete tuned gust, DTG. Two relevant magnitudes, wing root bending moment for a vertical DTG and VTP root bending moment for a lateral DTG are shown.

Top graphs show the two magnitudes transient response versus time. Mid and bottom graphs show the PSD and Accumulated PSD versus frequency, where it can be observed that all the response is produced at low frequency.

The peak in PSD graphs corresponds to the normal mode which is contributing the most to the response, 1st wing bending (symmetric) for the wing root bending moment and HTP yaw + Fuselage bending (antisymmetric) for the VTP root bending moment. These mode shapes are shown in Figure 5.

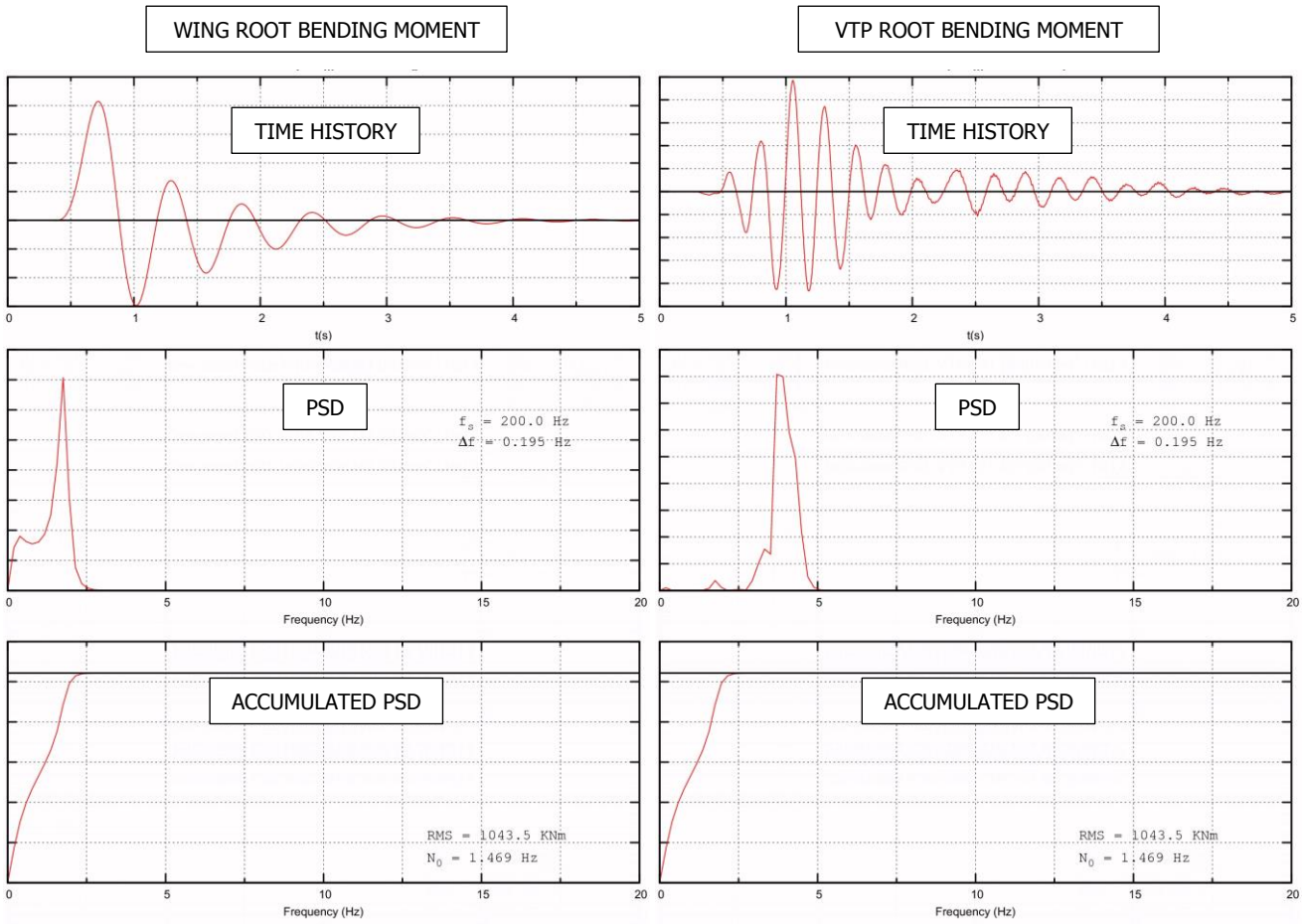

Figure 4: Heavy Military Transport A/C response to a DTG. Time history and PSD

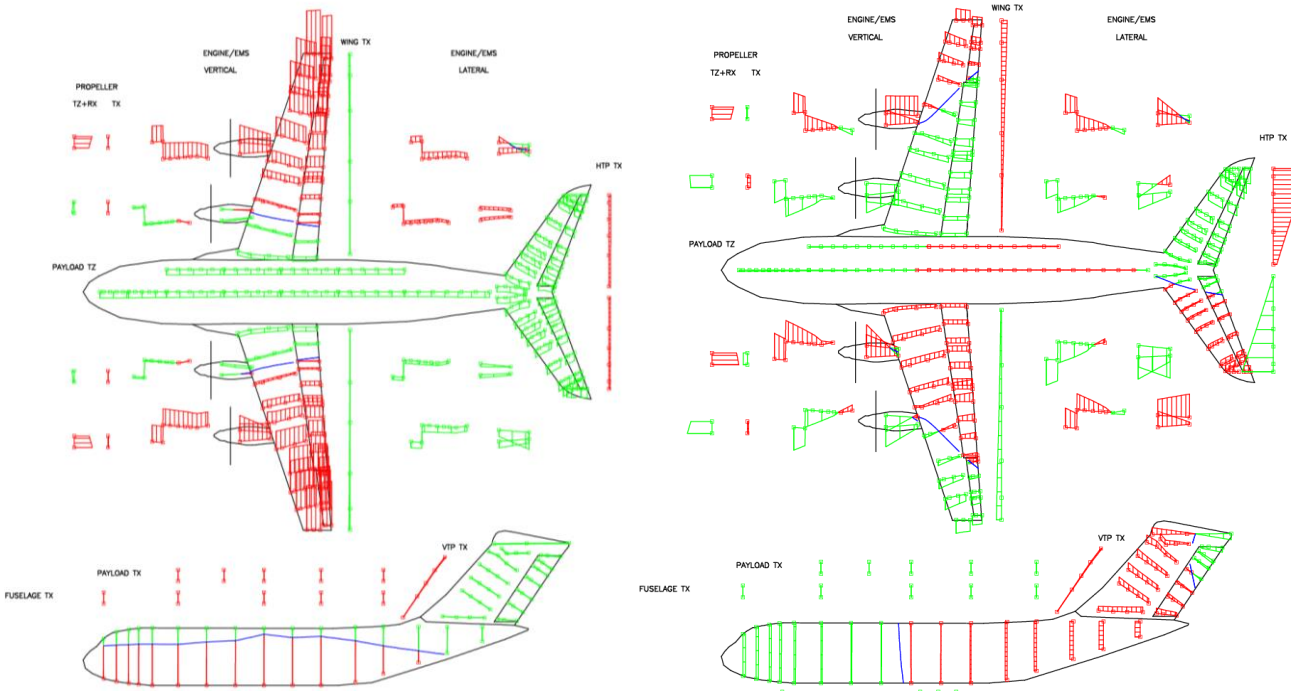

Figure 5: Heavy Military Transport A/C normal mode shape
Left:1st wing (S) bending (2 nodal lines) – Right: HTP yaw + Fuselage lateral bending

4 AIRCRAFTS NORMAL MODES AND THEIR RELEVANCE

4.1 Aircrafts normal modes shapes and frequencies

The mesh, geometry, connectivities and properties embodied in classical aircraft FEM models make them suitable to represent the dynamic behaviour of the structure at least up to 50. Hz. Nevertheless, commercial and military aircrafts dynamic loads and aeroelasticity events are typically driven only by a reduced set of low-frequency modes, usually with frequencies lower than 20. Hz. Table 1 shows the tanker MRTT first 50 modes identification and, amongst them, the 22 modes which are responsible for most of the dynamic or aeroelastic phenomena.

no.	MODE SHAPE DESCRIPTIONS	S/A
1-6	Rigid body modes	S/A
7	2N Wing Bending	S
8	3N Wing Bending	A
9	Ant. Engine Lateral	A
10	Sym. Engine Lateral	S
11	Rear Fuselage Lateral Bending	A
12	Sym. Engine Vertical	S
13	Ant. Engine Vertical	A
14	2N Fuselage Vertical Bending	S
15	HTP Roll	A
16	4N Wing Bending	S
17	2N Fuselage Lateral Bending	A
18	2N Wing Fore & Aft	S
19	Ant. Engine Roll & Yaw	A
20	Sym. Engine Roll & Yaw	S
21	5N Wing Bending	A
22	2N HTP Bending	S
23	1N VTP Bending	A
24	HTP Yaw (out of phase with fuselage)	A
25	HTP Yaw (in phase with fuselage)	A
26	6N Wing Bending	S
27	Fuselage Torsion	A
28	3N Fuselage Vertical Bending	S
29	Ant. Wing torsion	A
30	Sym. Wing torsion	S
31	2N VTP Bending	A
32	7N Wing Bending	A
33	Sym. Winglet Bending	S
34	8N Wing Bending	S
35	FRU Lateral	A
36	VTP Fore & Aft	S
37	Sym. HTP Fore & Aft	S
38	Ant. Pod Lateral	A
39	Rudder rotation	A
40	Sym. Pod Lateral	S
41	HTP torsion	A
42	Ant. Winglet Bending	A
43	Sym. Elevator rotation	S
44	Ant. Elevator rotation	A
45	Sym. Winglet Bending	S
46	VTP and Rudder Tip Bending	A
47	Ant. Pod Yaw	A
48	Sym. Pod Yaw	S
49	Ant. Aileron rotation	A
50	Sym. Aileron rotation	S

relevant

< 20Hz

no.	MODE SHAPE DESCRIPTIONS	S/A
7	2N Wing Bending	S
8	3N Wing Bending	A
11	Rear Fuselage Lateral Bending	A
14	2N Fuselage Vertical Bending	S
16	4N Wing Bending	S
17	2N Fuselage Lateral Bending	A
18	2N Wing Fore & Aft	S
21	5N Wing Bending	A
22	2N HTP Bending	S
23	1N VTP Bending	A
26	6N Wing Bending	S
28	3N Fuselage Vertical Bending	S
29	Ant. Wing torsion	A
30	Sym. Wing torsion	S
32	7N Wing Bending	A
37	Sym. HTP Fore & Aft	S
39	Rudder rotation	A
41	HTP torsion	A
43	Sym. Elevator rotation	S
44	Ant. Elevator rotation	A
49	Ant. Aileron rotation	A
50	Sym. Aileron rotation	S

Table 1 Tanker A/C first fifty normal modes and relevant modes selection

The typical normal modes shapes representations are 2D views, showing the nodal lines and projecting the relevant components displacements outside of the A/C shape, or 3D views, more intuitive and easy to understand but with the drawback that some details may be missed.

Figure 6 shows the MRTT 1st wing symmetric bending and Figure 7 shows the MRTT Aileron antisymmetric rotation. The first is, probably, the most important mode for dynamic loads, contributing to the response to Dynamic Landing, Taxi and Turbulence, which are often dimensioning the wing. The second mode is one of those involved in the Aeroelastic dynamic instabilities as lifting and control surfaces flutter mechanisms.

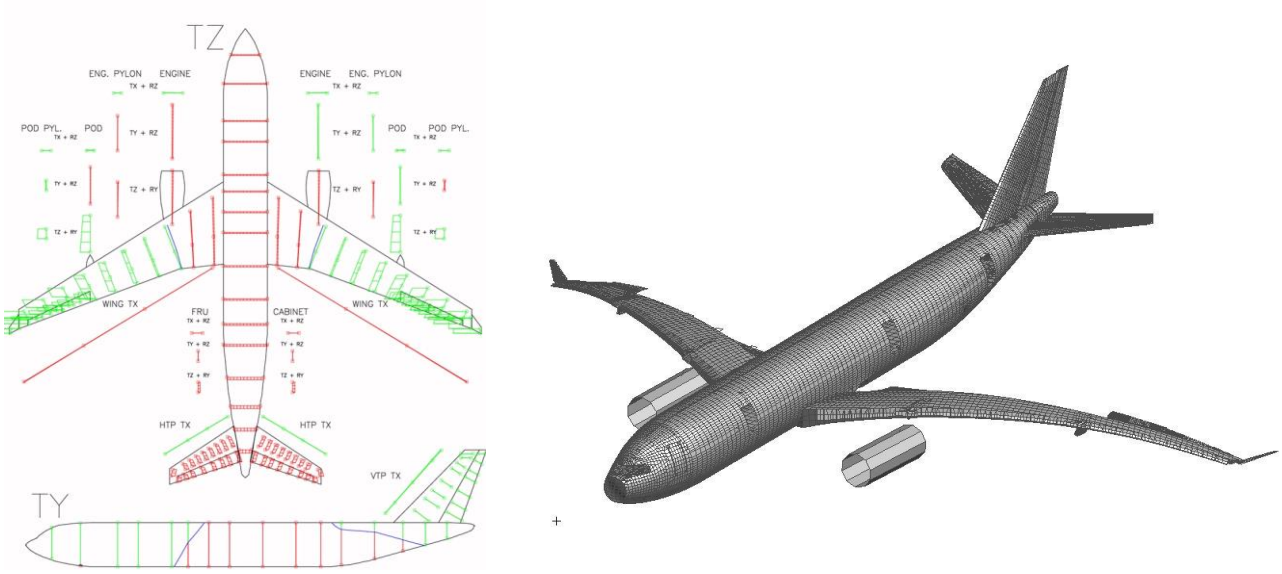

Figure 6: Tanker A/C normal modes. 1st wing (S) bending (2 nodal lines)

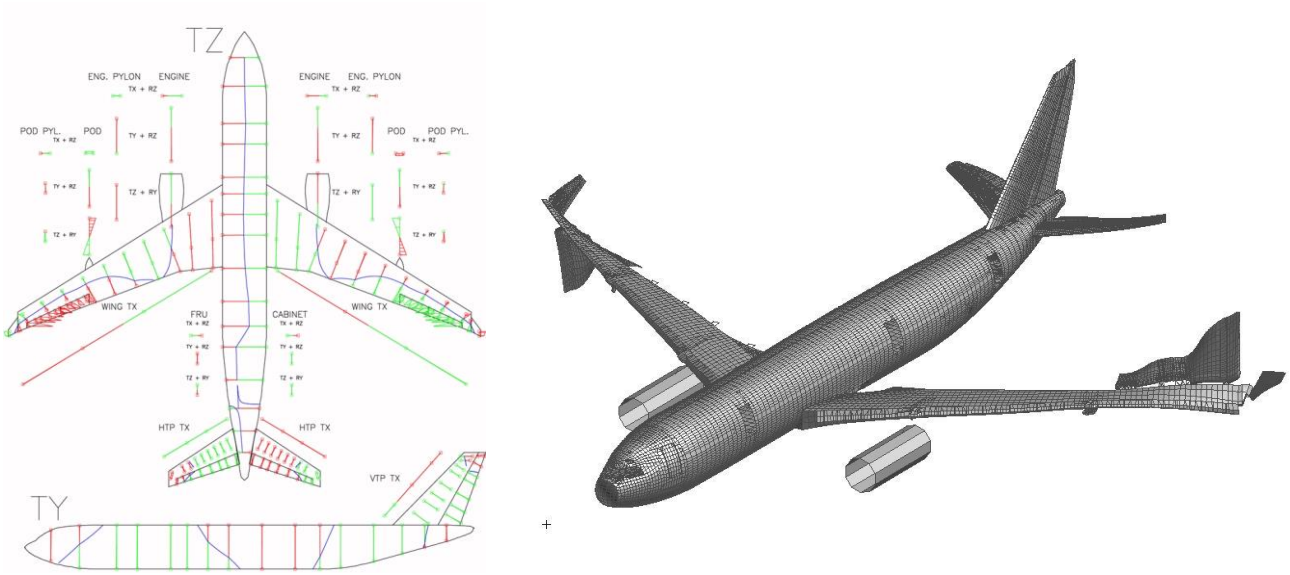

Figure 7: Tanker A/C normal modes. Aileron (A) rotation

4.2 Aircraft normal modes relevant for Dynamic Loads

Some aircraft scenarios provoke transient excitations:

- On ground: dynamic landing, taxi, nose wheel imbalance, etc.
- In flight: discrete tuned gust, continuous turbulence, buffet, etc.

With the exception of buffet, which may exhibit mid-high frequency contents, the rest of dynamic loads scenarios excitations have a frequency contents that rarely exceeds 10-15 Hz. Therefore, only the aircraft lower frequency modes will be excited by these transient loads. Amongst the low frequency modes, those contributing the most to the dynamic loads are:

- 1st wing bending
- 1st wing torsion
- 1st Horizontal Tailplane bending
- 1st Vertical Tailplane bending
- 1st fuselage bending

How are these modes? Where are their natural frequencies?

As a general principle it can be stated that the heavier and the more flexible aircrafts are, the lower normal modes frequencies they have. But there are other characteristics, such as wing sweep, span, engine location or tail position which affect the normal modes frequencies.

This section is a compilation of the typical aircrafts families' most relevant normal modes frequencies, emphasizing differences and similarities of the different aircrafts types: Commercial narrow body and wide body, Military Transport Light to Heavy, Fighter or Trainer. In all the figures, the frequency in Hz is represented versus the Maximum Take-off Weight (MTOW) in tonnes. For each aircraft type or family, the vertical bars representing the frequency copes with the different mass status (payload/fuel distribution), from OWE to MTOW.

Figure 8 shows the 1st wing bending modes for the different aircrafts families. In general, the lighter the aircraft, the higher the frequency; Fighter delta wings (top graph) have higher bending frequencies than M&L aircrafts with similar MTOW (centre graph), and straight wing frequencies (centre graph), are higher than rearward-swept wings ones (bottom graph). The fuel contents in the wing or the fighter underwing stores make the frequencies to decrease.

The wing torsion is less affected by the wing fuel contents, as it can be seen in Figure 9. Low-weight and straight-wings aircrafts are usually stiffer in torsion, thus having higher frequencies. The Fighter (top graph) is a particular case in which wing torsion frequency has a big variation due to its delta wing and wide variety of underwing external stores.

Horizontal and vertical tails bending modes behaviour are similar to the wing ones: the heavier the aircraft, the large and more flexible the tails and therefore, the lower the frequencies. Figure 10 and Figure 11 show two particularities:

- For commercial aircrafts (Figure 10 bottom graph) trimmed with HTP fuel tanks, the HTP bending frequency shows a range of variation. This variation is associated to the different fuel contents.
- The Heavy Transport with T-tail has much lower VTP bending frequency than the similar size aircrafts with standard tail (Figure 11 mid and bottom graphs).

As shown in Figure 12, behaviour of all aircrafts in terms of fuselage vertical bending is similar to the one observed in wing and HTP components: small aircrafts are stiffer, with higher frequencies, while large commercial ones are more flexible, with lower frequencies. Contrary to what could be expected, bottom graph heaviest wide body aircraft has higher frequency than the trend shown by the rest of wide body aircrafts, due to its relatively shorter length and larger cross-section for its double deck.

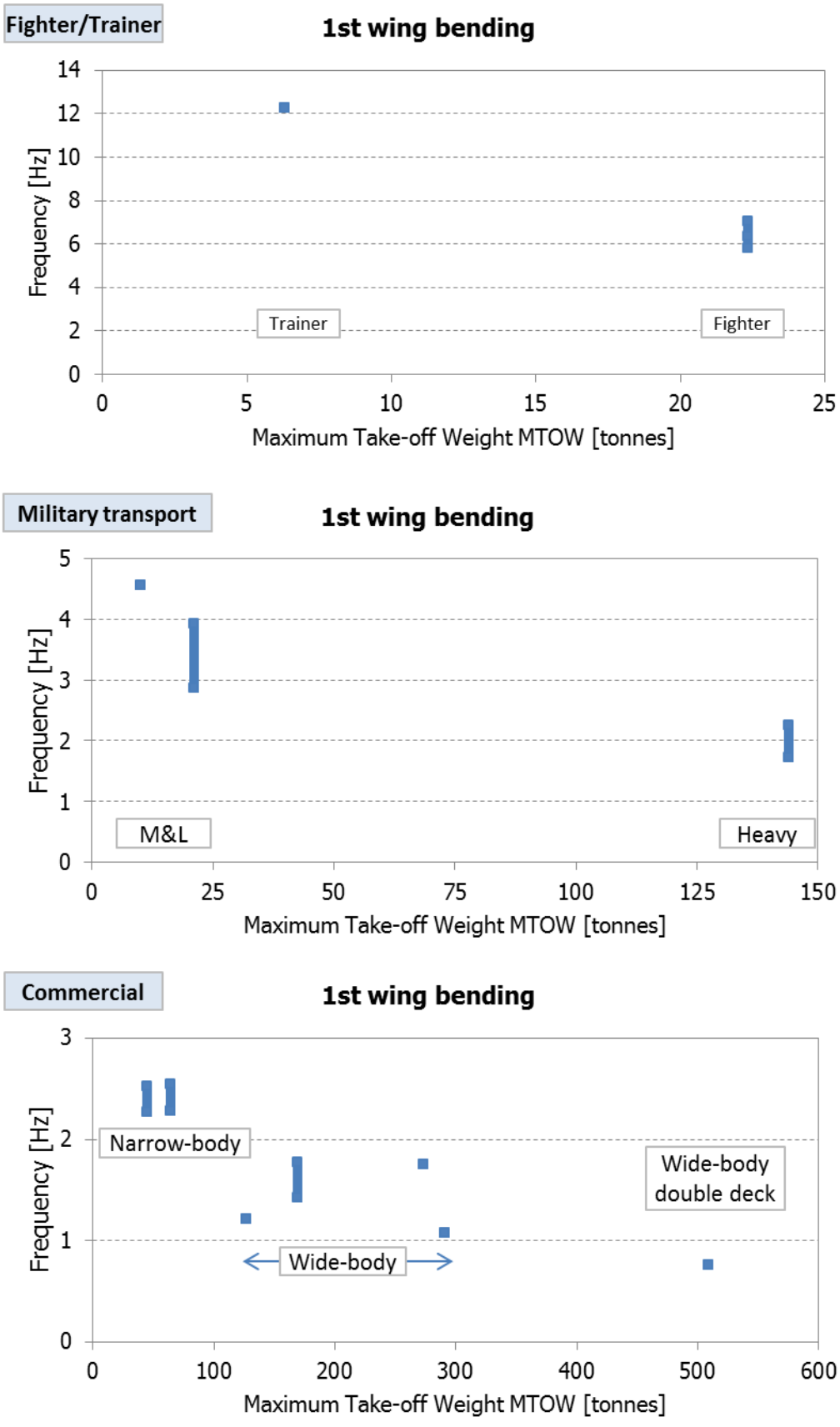

Figure 8: 1st wing bending normal mode frequency vs MTOW

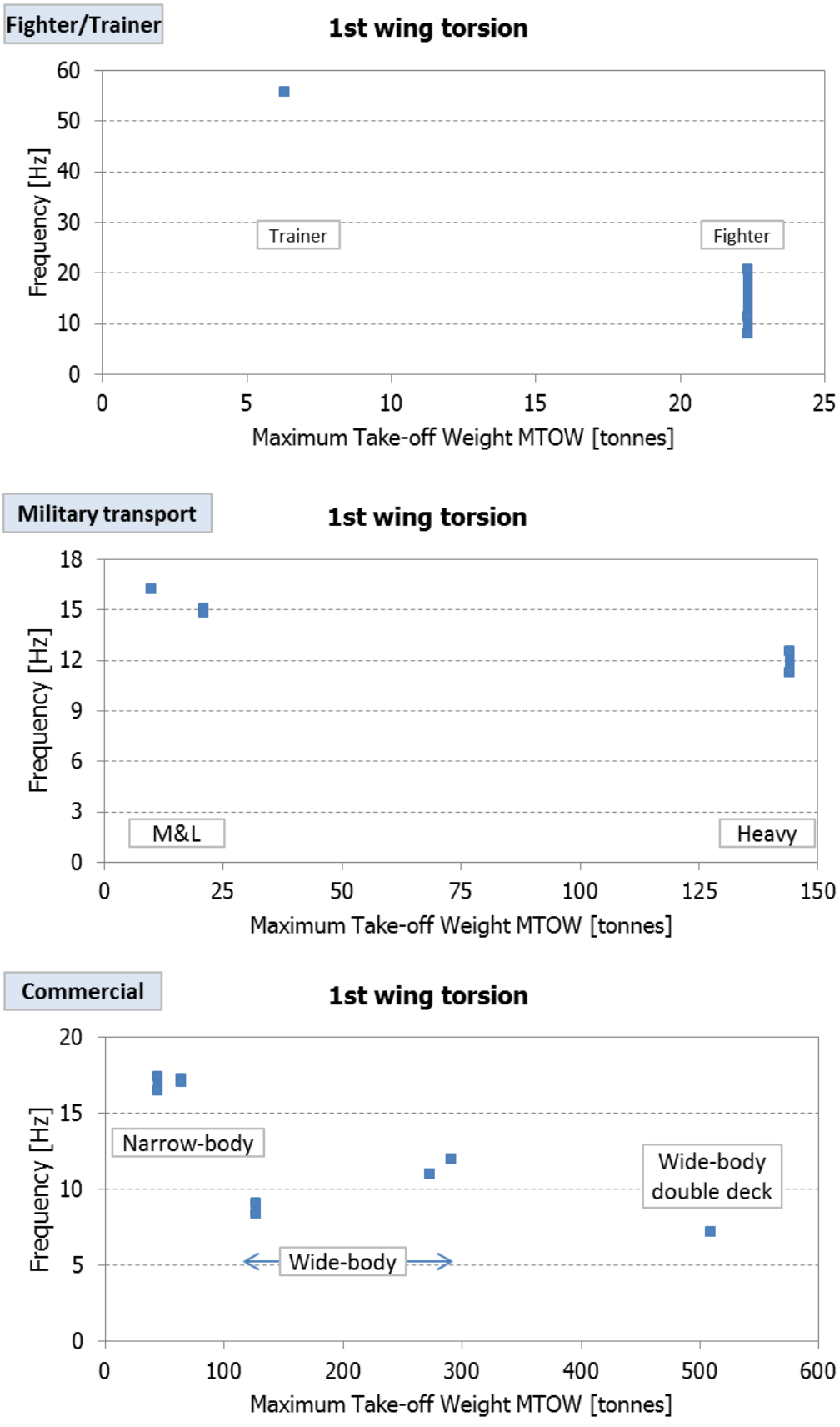

Figure 9: 1st wing torsion normal mode frequency vs MTOW

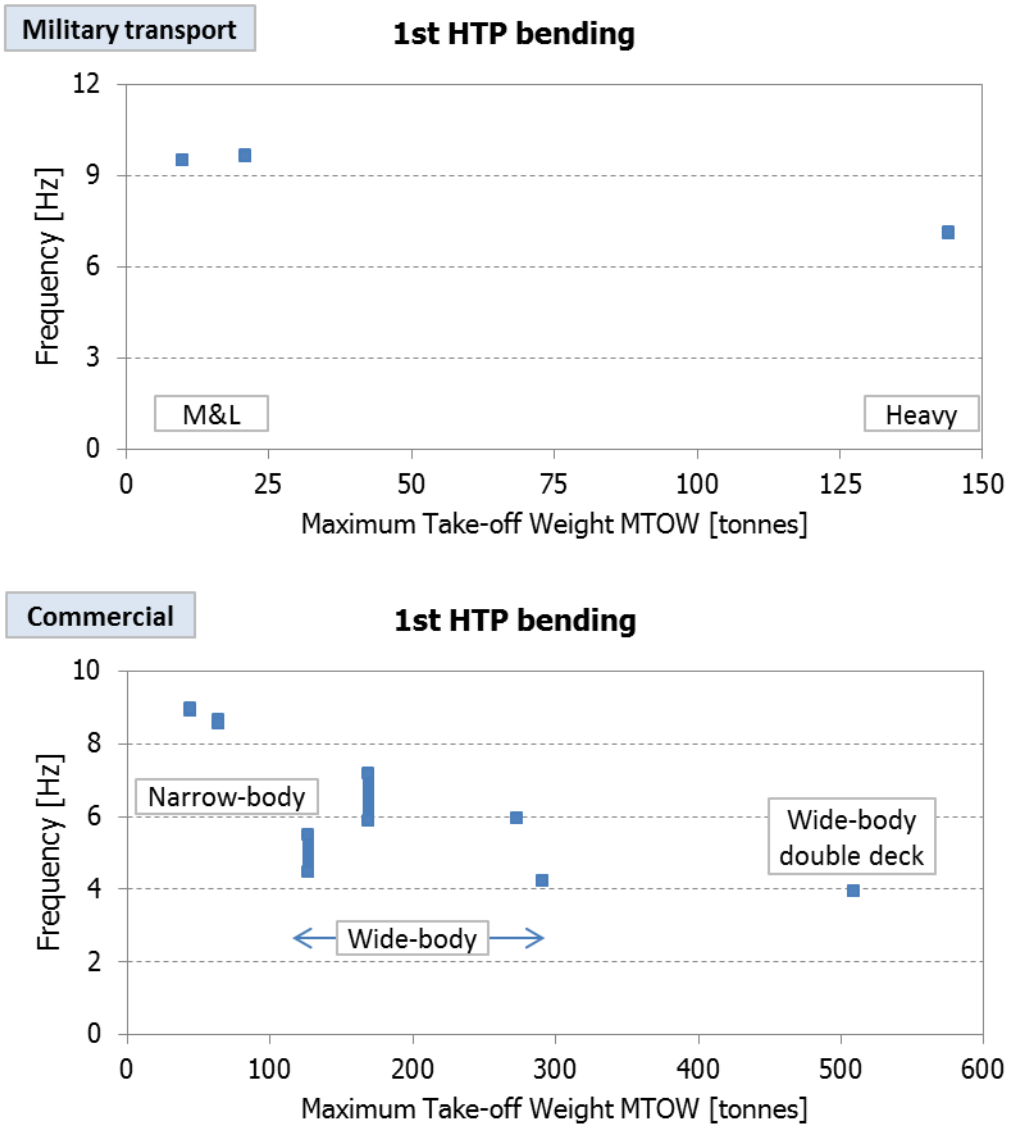

Figure 10: 1st HTP bending normal mode frequency vs MTOW

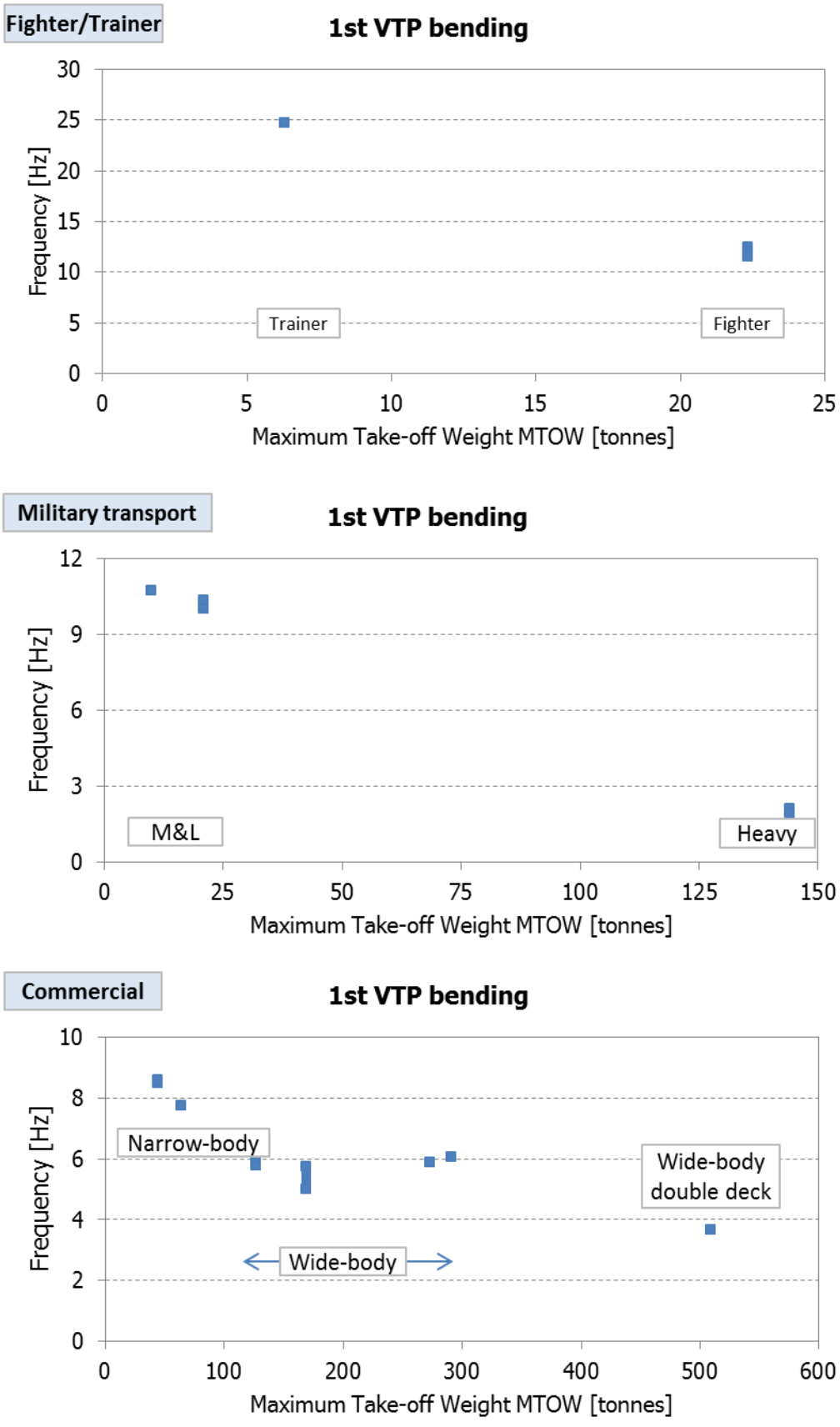

Figure 11: 1st VTP bending normal mode frequency vs MTOW

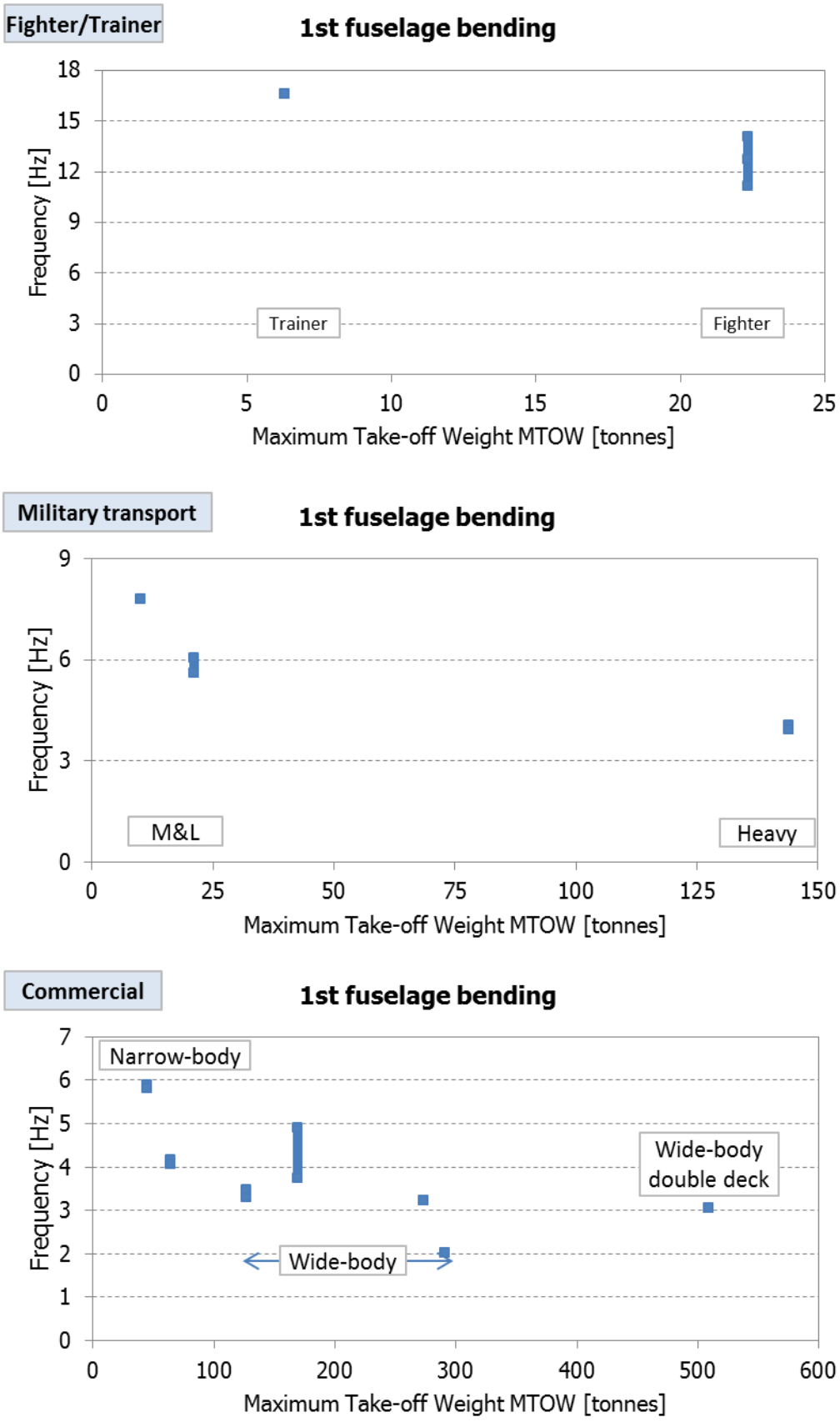

Figure 12: 1st fuselage bending normal mode frequency vs MTOW

4.3 Additional aircrafts normal modes relevant for Aeroelasticity

In addition to the low frequency modes shown in previous section, there is a group of modes also relevant for aeroelasticity: the control surface rotation modes.

Basically, control surfaces may be actuated in two ways:

1. Manual controls, i.e., direct wires between the control column in the cockpit and the control surface.
2. Controls with actuators.

For manual controls, the control surface rotation mode frequency is roughly zero Hz; friction makes this frequency to be slightly above zero.

For controls with actuators, the control surface rotation mode frequency lies in the range 10 to 20 Hz, depending mainly on the control surface size.

Figure 13 shows the effect of the aircraft controls type on the control surfaces rotation frequency for a wide variety of military and commercial aircrafts.

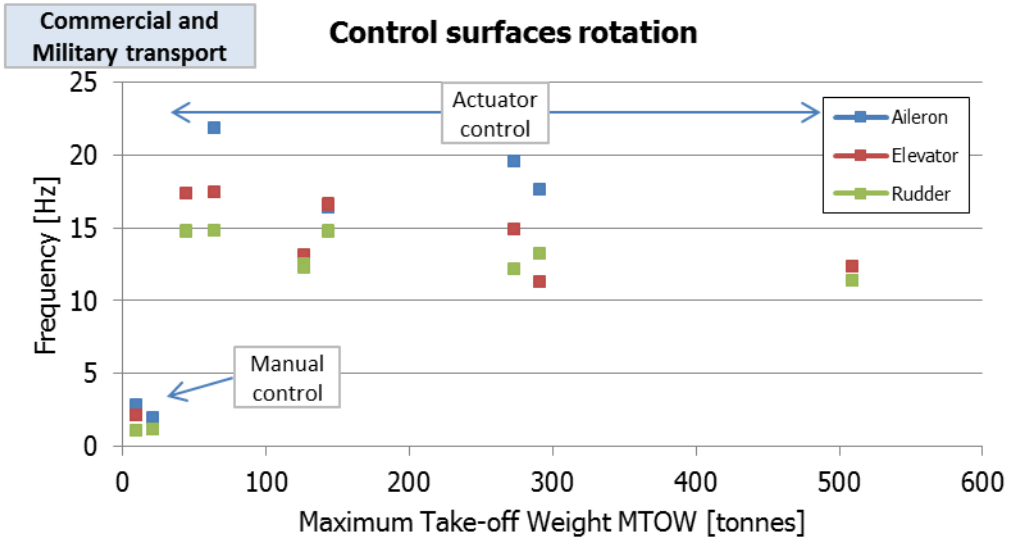

Figure 13: Control surfaces rotation vs MTOW

Control surface flutter mechanism is typically consequence of the lifting surface bending and the control surface rotation modes coupling. The control surfaces actuators stiffness is a driving parameter for those modes, affecting not only to its rotation mode frequency but also to its mode shape.

In order to better understand the flutter mechanism, sensitivity analyses to this stiffness are performed during the design phase. The flutter behaviour in an actuator failure case and the actuator tolerances have also to be assessed in the certification phase.

Figure 14 shows a commercial aircraft normal modes frequencies evolution when reducing its L/H actuator nominal stiffness to a value close to its disconnection in five steps:

1. Both aileron actuators nominal stiffness ($K_{R/H}$= $K_{L/H}$=K_{NOM}).
   - Pink curve: Ailerons symmetric rotation. Nominal frequency, same as antisymmetric.
   - Dark blue curve: Ailerons antisymmetric rotation. Nominal frequency, same as symmetric.
   - Green curve: 1st wing symmetric bending. Nominal frequency.
     Mode shapes: Ailerons modes show certain torsion along their span. Wing mode is a pure uncoupled bending mode. See also Figure 15.
2. L/H aileron actuator stiffness reduced one order of magnitude and R/H aileron actuator stiffness remains unchanged ($K_{L/H}$↓, $K_{R/H}$= K_{NOM}).
   - Pink curve: L/H Aileron rotation at a frequency lower than the nominal one.

- Dark blue curve: R/H Aileron rotation at the nominal frequency.
- Green curve: 1st wing symmetric bending. Nominal frequency.
  Mode shapes: Two uncoupled R/H and L/H ailerons rotation modes instead both sides symmetric and antisymmetric. Both modes show certain torsion along their span. Wing mode is a pure uncoupled bending mode.

3. L/H aileron actuator stiffness reduced two more orders of magnitude and R/H aileron actuator stiffness remains unchanged ($K_{L/H}\downarrow\downarrow$, $K_{R/H}= K_{NOM}$).
   - Pink curve: L/H Aileron rotation at a frequency close to the than the 1st wing symmetric bending one.
   - Dark blue curve: R/H Aileron rotation at the nominal frequency.
   - Green curve: 1st wing symmetric bending. Nominal frequency.
     Mode shapes: R/H aileron mode shows certain torsion along its span. L/H aileron rotation mode is a pure rotation mode. Wing mode is coupled with the aileron rotation.
4. L/H aileron actuator stiffness reduced one more order of magnitude and R/H aileron actuator stiffness remains unchanged ($K_{L/H}\downarrow\downarrow\downarrow$, $K_{R/H}= K_{NOM}$).
   - Pink curve: L/H Aileron rotation at a frequency between flexible modes and rigid body modes.
   - Dark blue curve: R/H Aileron rotation at the nominal frequency.
   - Green curve: 1st wing symmetric bending. Nominal frequency.
     Mode shapes: Same as step 3.
5. L/H aileron actuator stiffness reduced to a value close to zero and R/H aileron actuator stiffness remains unchanged ($K_{L/H}\approx 0$, $K_{R/H}= K_{NOM}$).
   - Pink curve: L/H Aileron rotation at a frequency close to zero (rigid body mode).
   - Dark blue curve: R/H Aileron rotation at the nominal frequency.
   - Green curve: 1st wing symmetric bending. Nominal frequency.
     Mode shapes: Same as step 3. See also Figure 15.

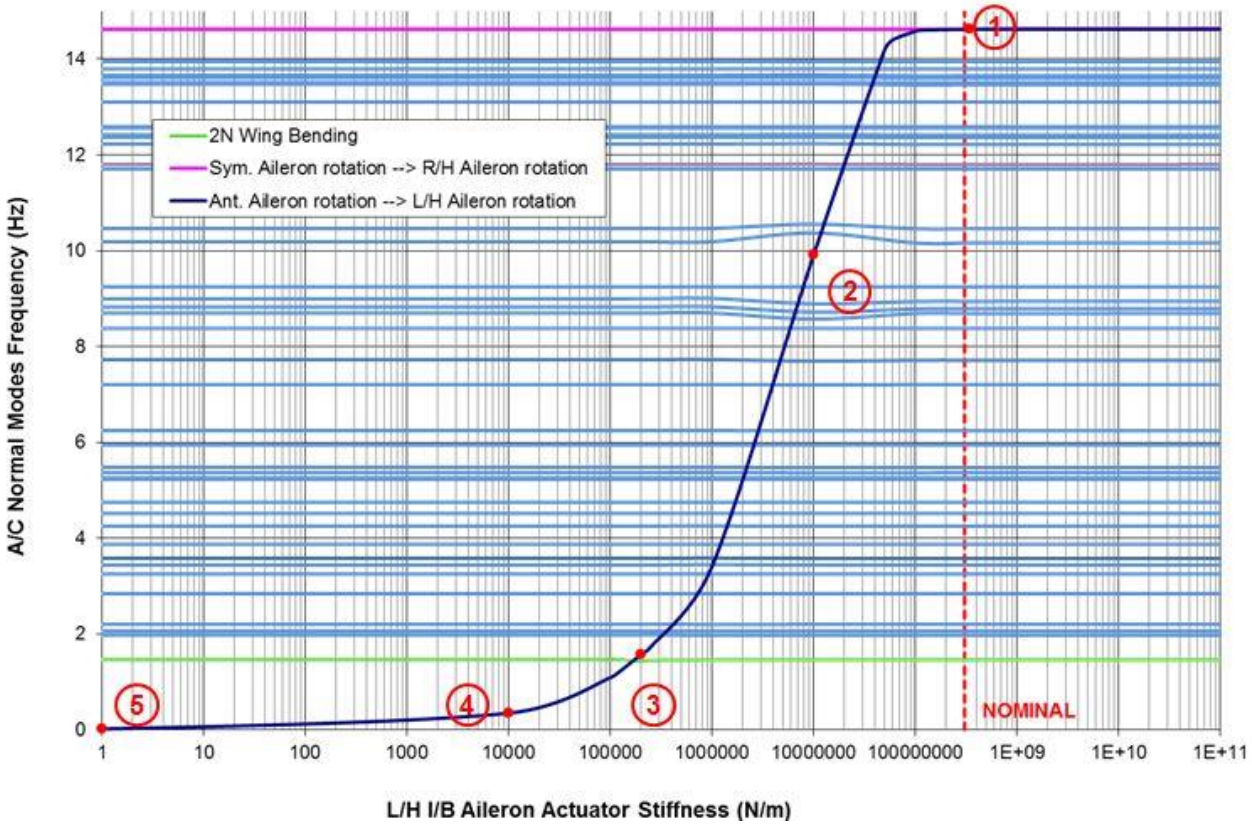

Figure 14: Commercial A/C - Normal modes frequency sensitivity to one-side aileron actuator stiffness

Figure 15 shows the change in the aileron and wing bending normal modes: With the actuator nominal stiffness (left hand plots) the wing bending is an uncoupled mode and the ailerons rotation shows a degree of torsion along its span. When reducing the actuator stiffness to a value close to disconnection (right hand plots), the wing bending mode is coupled with the L/H aileron rotation, which on its part is a rotation rigid body mode.

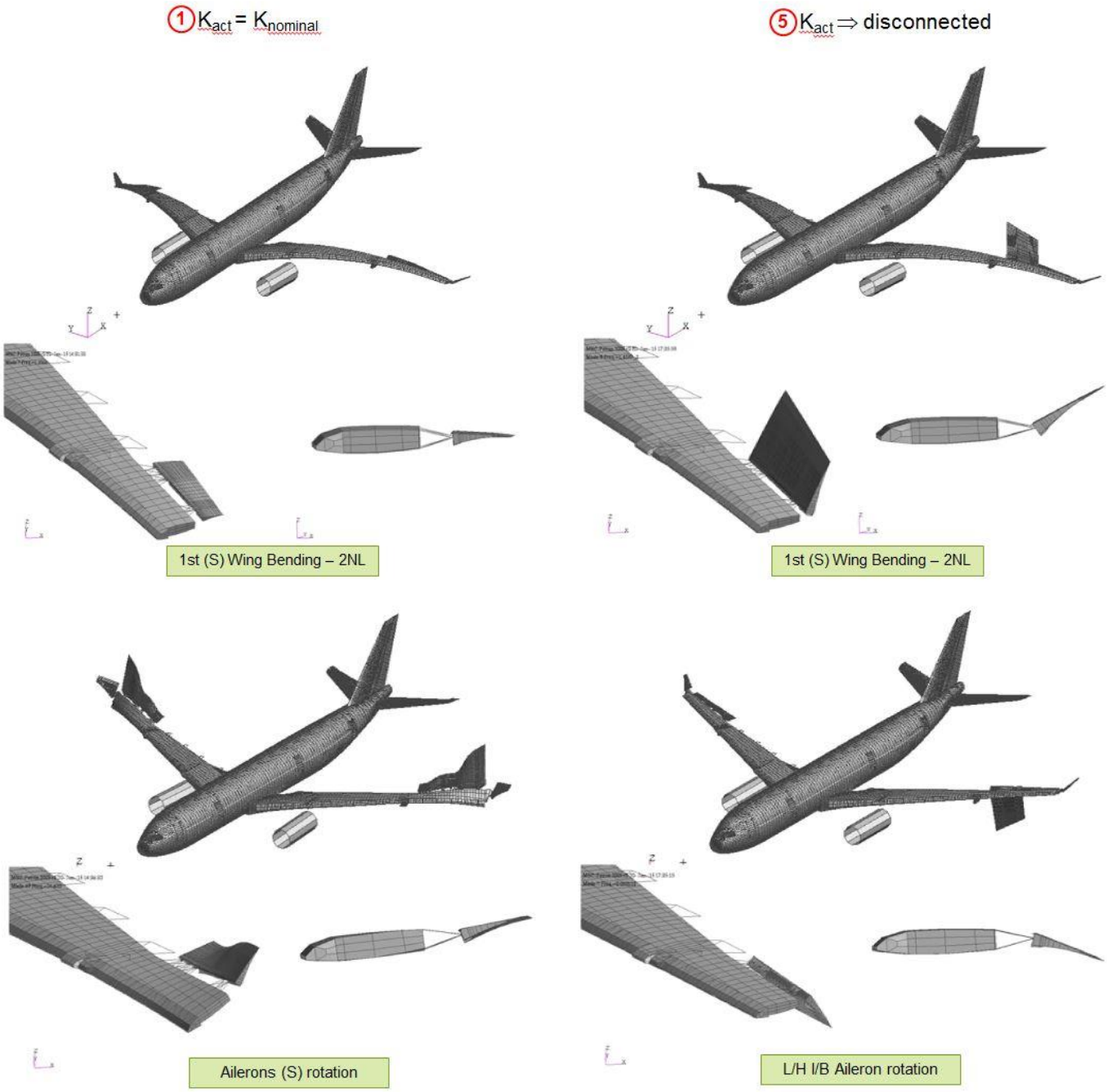

Figure 15: Commercial A/C - Normal modes shapes sensitivity to one-side aileron actuator stiffness

4.4 How to alter the bending – control rotation coupling through mass balance

Mass balance is often used to prevent the lifting and control surface flutter. For this purpose, high density material weights (e.g. lead, tungsten, etc.) are added either to the control surface or to the torsion box, depending on the nature of the control system and on the modes coupling to be avoided:

- In **manual control** by wires, the mass is added to the control surface in order to move its centre of gravity ahead the hinge line. When the wing bends up the control surface rotates up leading to a negative aerodynamic force that reduces the wing bending. The mass is added to the torsion box in order to change the phase between the control surface rotation and the wing bending motion
- In **controls with actuators**, the mass balances is to change the mode shapes and frequencies, thus de-coupling the potential flutter modes.

Figure 16 shows the effect of balance mass added in a classical flutter of control surface with actuators coupling with lifting surface bending.

Left hand graph shows the structure normal modes damping and frequency evolution with the A/C speed. Mode 1, lifting surface bending, couples with mode 2, control surface rotation, as their frequencies approach with the speed increase. Mode 1 damping drops thus becoming unstable when crossing the zero damping line.

Right hand graph shows the effect of the balance mass added to the torsion box tip: the frequencies split and separate and the lifting surface bending damping increases. For a certain amount of mass, the mode does not cross the zero damping line and no flutter appears at any speed. The blue arrows show the sense of increasing balance mass.

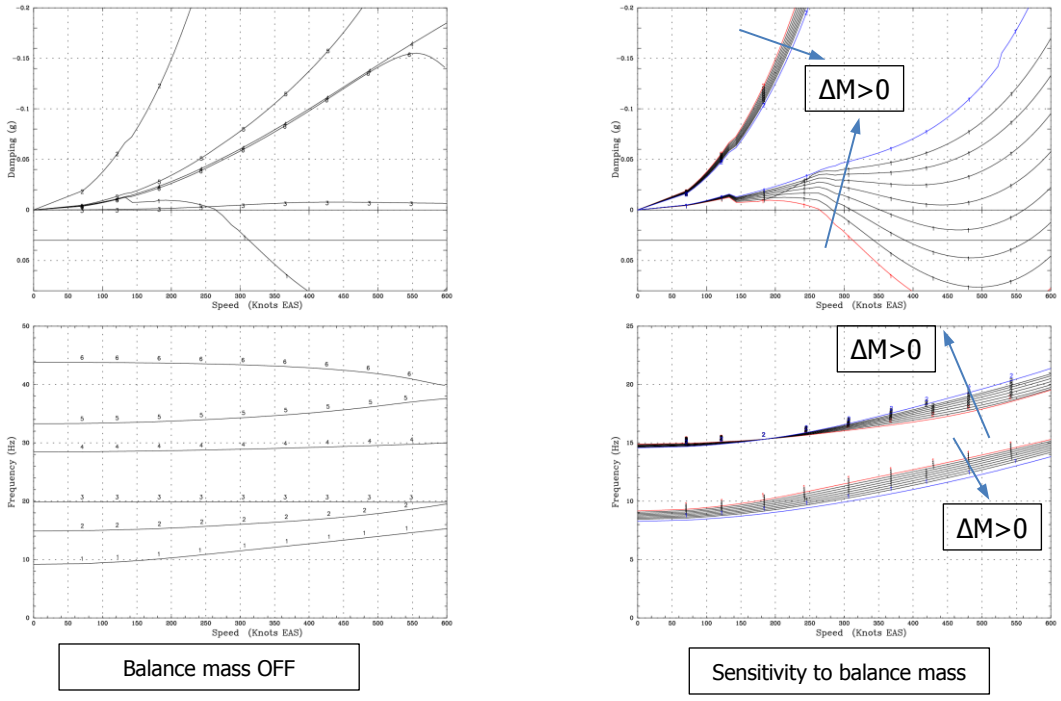

Figure 16: Classical flutter prevention by adding mass balance

5 STRUCTURAL DYNAMIC MODELS VALIDATION

5.1 General

Airworthiness regulations proof of compliance require the analytical results to be supported by ground and flight tests, [4]. This section briefly shows the most relevant aspects of the structural Finite Element dynamic models validation by Ground Vibration and Flight Tests, and the influence of non-linearities in the A/C normal modes and, consequently, in this validation.

5.2 Ground Vibration Tests

The Ground Vibration Tests objective is to obtain experimentally the normal modes of the complete aircraft and in particular:

- Frequencies & mode shapes.
- Damping & modal mass.
- Non-linearities (if any).

In turn, results are used to validate or update (if needed) the structure FEM model. Figure 17 shows a typical structural dynamic model validation flow chart.

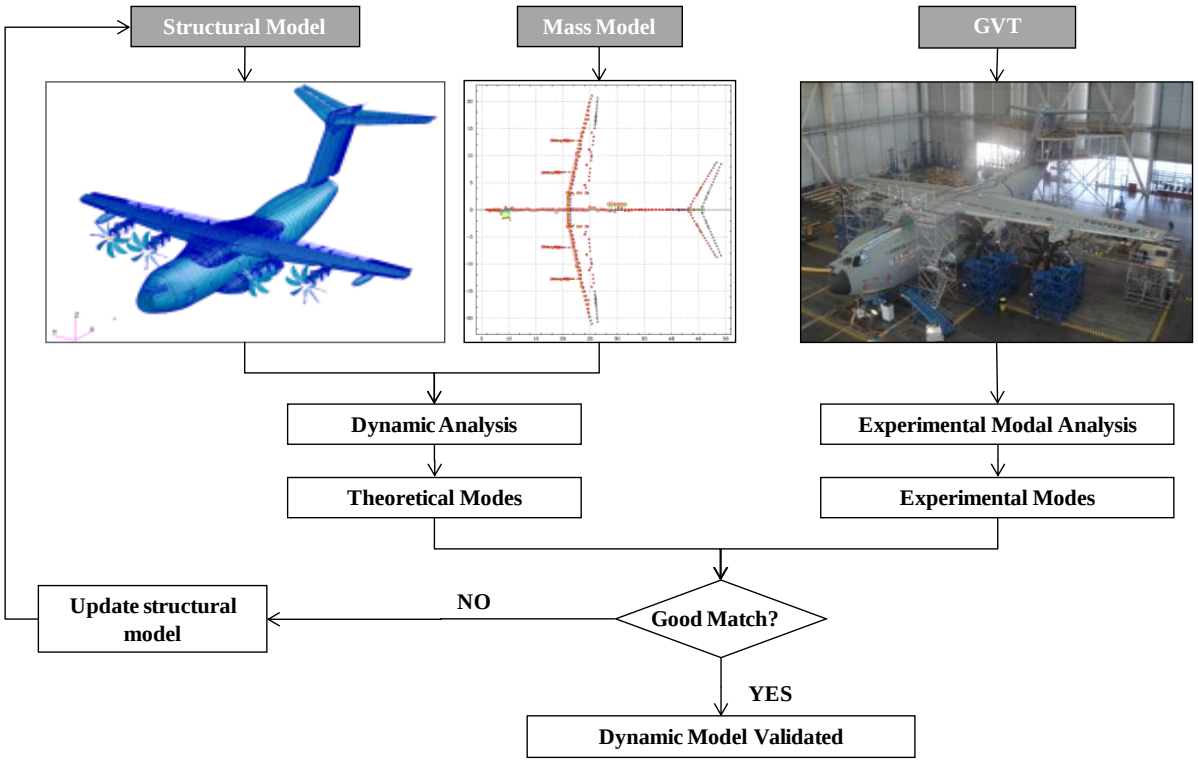

Figure 17: Commercial A/C flutter prevention by mass balance

GVT results are typically represented in a graph that compares theoretical modal frequencies (obtained from a FEM model, for instance) with experimental data. Ideally, test results should be aligned with the 45° division line (continuous red line of Figure 18). The closer these data are to that line, the better the model is behaving and fewer changes will be needed.

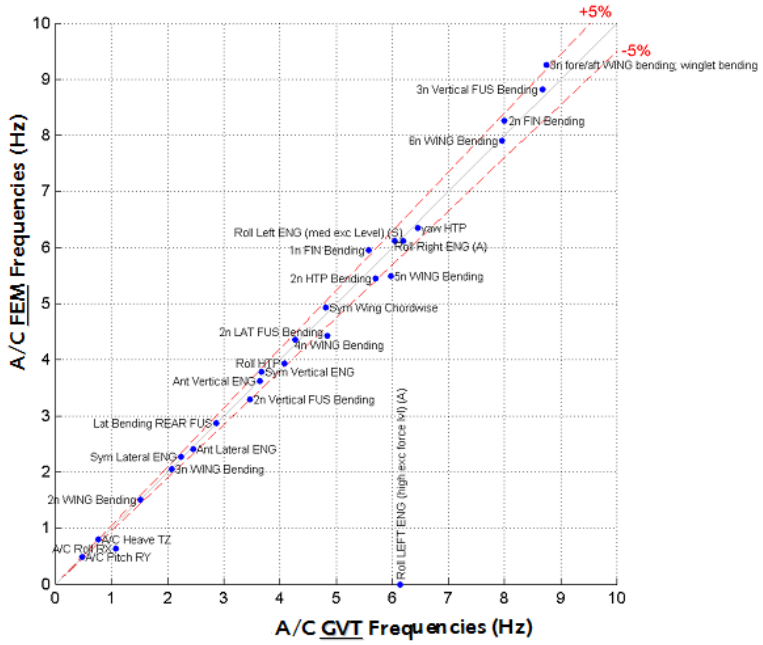

Figure 18: Typical GVT results plot

More information on the test instrumentation and execution, as well as the model validation and adjustment can be found in [5] and [6].

5.3 Flight Tests

During every aircraft Flight Test campaign, loads and accelerations are monitored and they are used not only to assess their peak values but also to extract from them the modal information which can be used to validate the aircraft models.

Figure 19 shows a typical dynamic ground loads model validation flow chart. After the landing gear validated by the drop and free extension tests and the structural dynamic model validated by the GVT, the landing gear coupling to the A/C structural model is validated by means of dedicated firm landing and taxi tests. In both cases the flow chart is similar: Flight test data are compared with the analytical results obtained with the integrated A/C-L/G model. The coupling model is adjusted if necessary and finally validated.

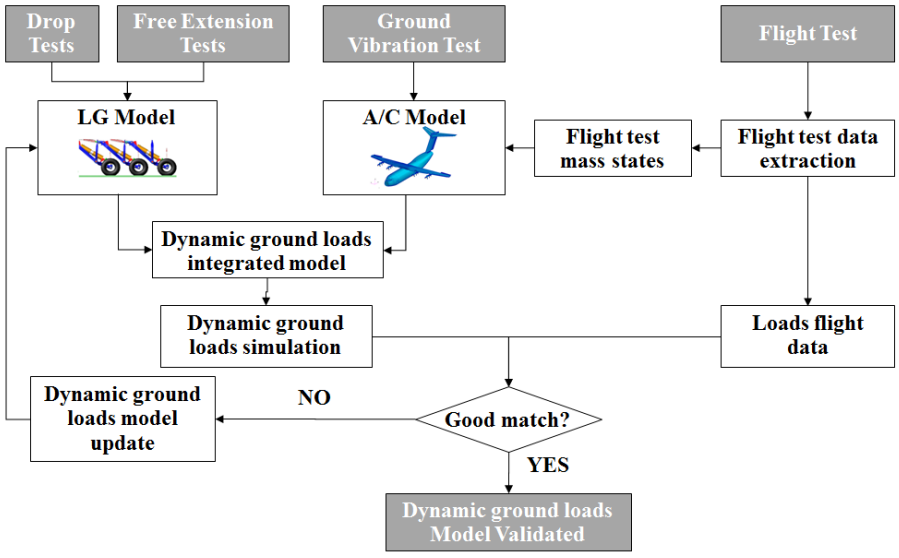

Figure 19: Dynamic ground loads model validation flow chart

Flight Flutter Tests are used to clear the A/C flight envelope and also check the modes frequency and damping evolution with speed, thus providing means to validate the flight dynamic loads and aeroelastic model. Figure 20 shows the model validation flow chart.

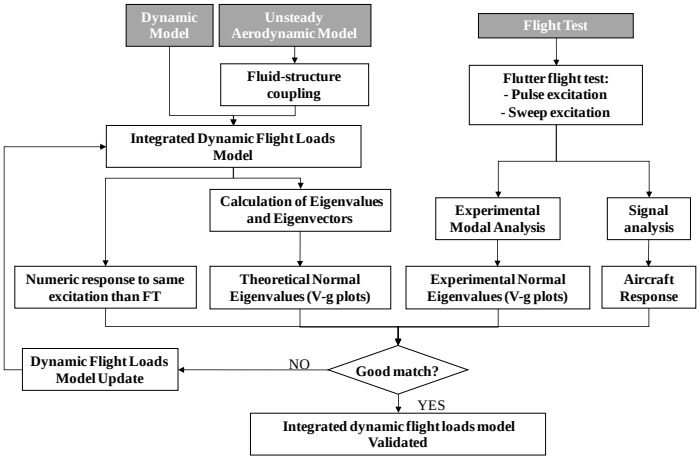

Figure 20: Heavy transport aircraft fight loads model validation flow chart

Figure 21 to Figure 25 show the comparison between the heavy transport aircraft flight tests and analytical results for a set of loads and accelerations. Results obtained in hard landing and taxi tests show good agreement. For a deeper discussion and more results, see [5].

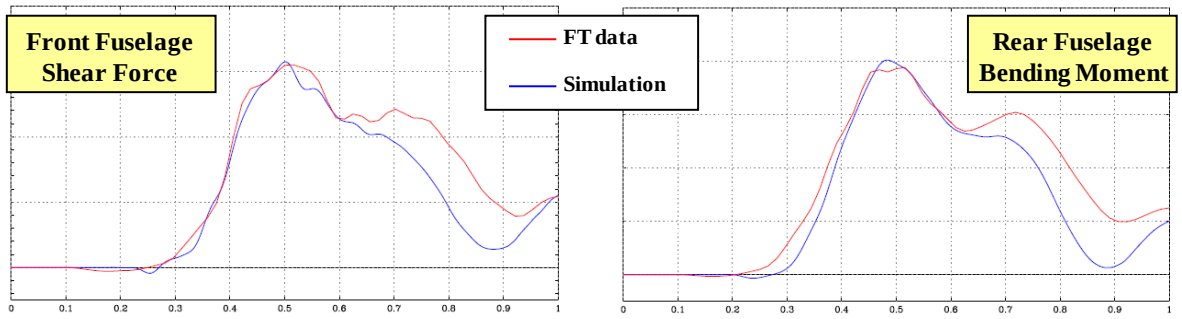

Figure 21: Heavy transport aircraft test-simulation loads comparison. 10.9 ft/s landing

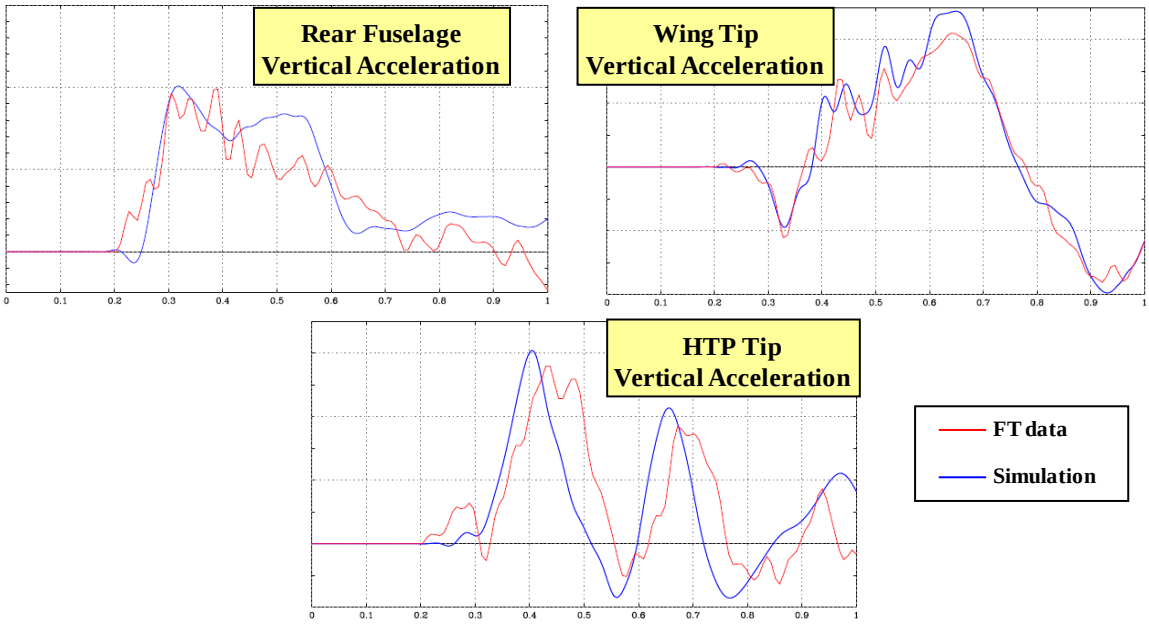

Figure 22: Heavy transport aircraft test-simulation accelerations comparison. 10.9 ft/s landing

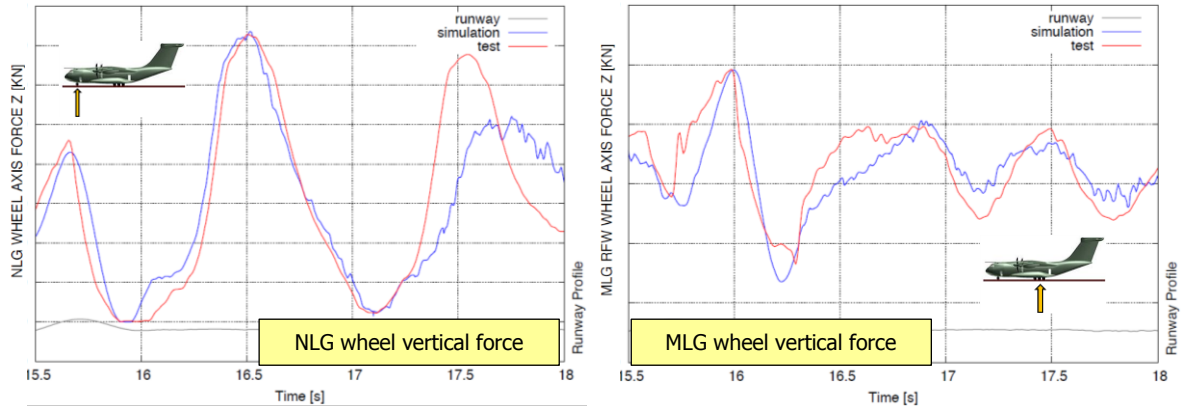

Figure 23: Heavy transport aircraft test-simulation LG loads comparison. Taxi over (1-cos) bump

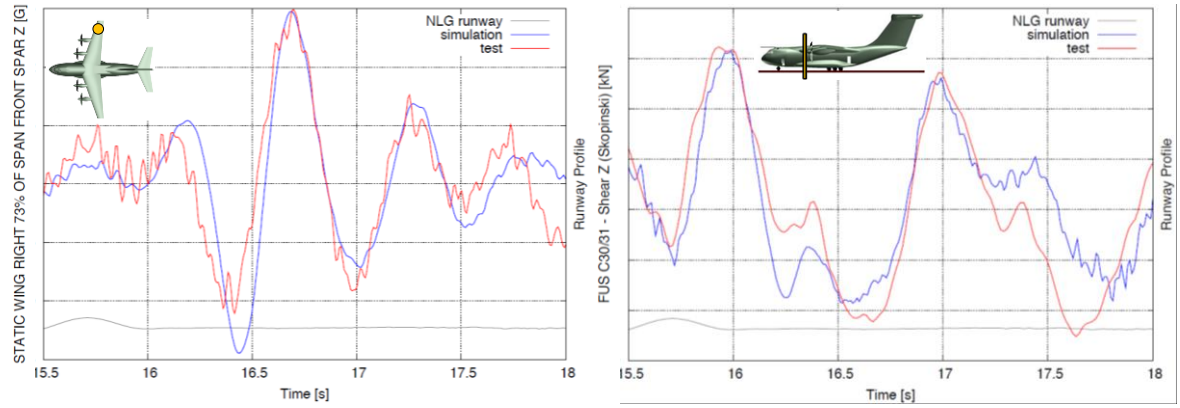

Figure 24: Heavy transport aircraft test-simulation comparison. A/C loads. Taxi over (1-cos) bump

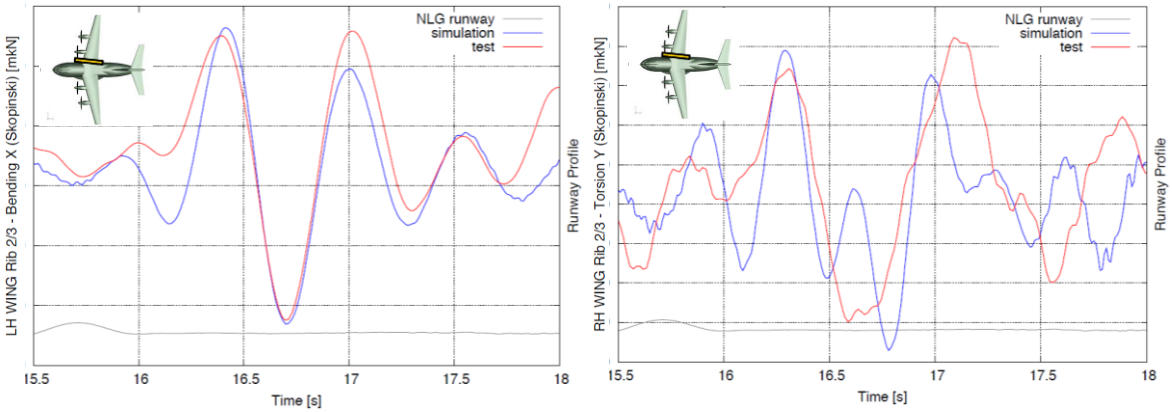

Figure 25: Heavy transport aircraft test-simulation comparison. A/C accelerations. Taxi over (1-cos) bump

Figure 26 and Figure 27 show the Flight Vibration Tests Results represented in form of the classical flutter V-g and V-f plots for the wing bending modes. Both, frequency and damping test results show good agreement with the theoretical analyses. The adjustment made to the theoretical damping at zero frequency is based on the GVT results, obtained for small displacements. Due to some A/C non-linearities, this is a conservative assumption.

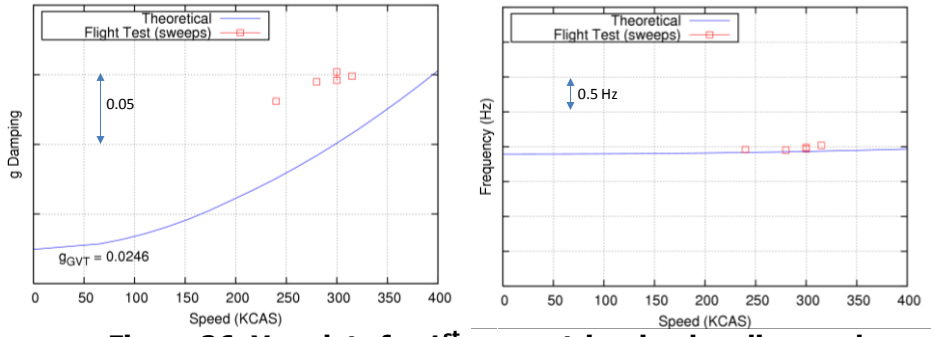

Figure 26: V-g plots for 1st symmetric wing bending mode

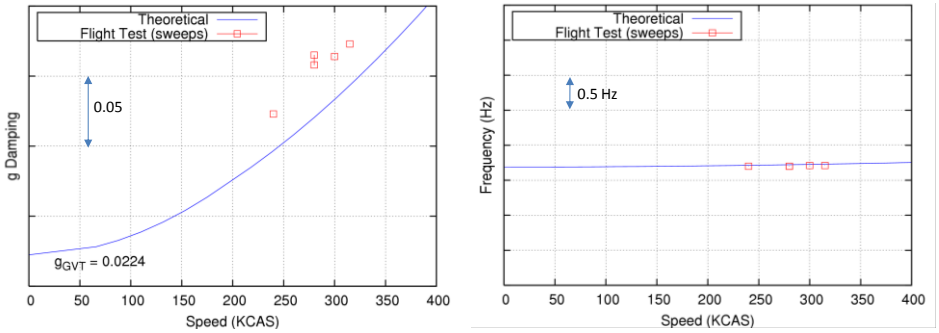

Figure 27: V-g plots for 1st antisymmetric wing bending mode

5.4 Effect of A/C non-linearities in normal modes

One of the eigenvalue technique basic assumptions is the system linearity. In some cases this assumption is valid close to the nominal conditions for which the dynamic model has been defined.

All real structures present some non-linear behaviour up to some extent. Significant sources of non-linearity in aerospace structures include riveted metallic construction, nacelle latches, hydraulic actuators of control surfaces (freeplay, hysteresis, or non-linear spring-type force) and elastomeric engine mounts.

As described in [6], the main footprint of non-linear effects affecting a vibrating structure is the variation of frequency peaks in the response to different levels of energy introduced into the structure. In many vibration tests, the increase of excitation force levels in order to corroborate the changes in those peaks is very common. Figure 28 shows an example of frequency peak variation with excitation force level and normal mode frequency and damping evolution with excitation force level.

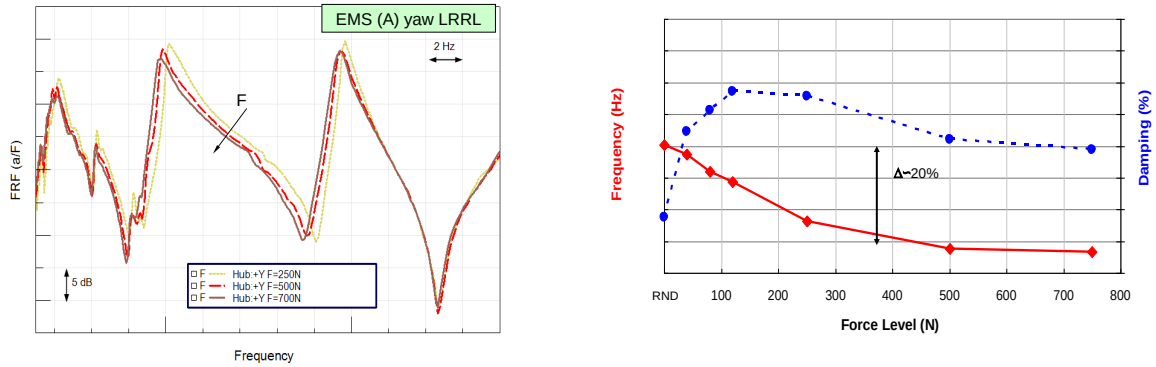

Figure 28: Driving point FRF's (left) and normal mode frequency and damping (right) for increasing excitation force level.

Secondary structures (fairings, some non-structural aircraft doors, etc.) are often conservatively excluded from checkstress models, which are usually the basis for structural dynamic models definition. These secondary structures may also contribute to a non-linear behaviour of the normal modes in a Ground Vibration Test. In the heavy transport aircraft GVT described in [6], the engine composite cowlings were identified as a possible source of non-linearity on the EMS modes. Engine cowls were removed and EMS normal modes measured for different excitation force levels in order to compare with COWLS-ON cases. Measured results for EMS Roll mode (Figure 29) confirmed this statement. It could be appreciated a stabilization of EMS roll mode from medium excitation levels, whereas COWLS-ON case had not shown normal mode stabilization at the highest excitation forces reached on GVT.

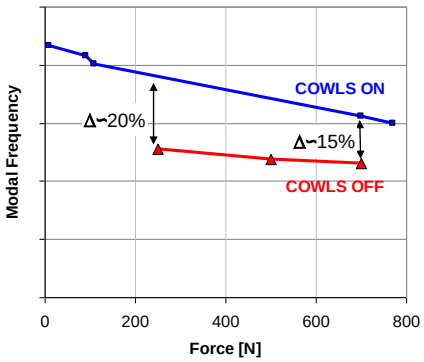

Figure 29: Cowling removal effect on EMS Roll mode.

Other non-linear effect is the structure high-flexibility, which affects its normal modes frequencies in a similar way as the violin string tuning.

By performing non-linear normal modes calculation for a highly flexible aircraft it can be predicted this behaviour. Figure 30 shows the effect of the applied load (from -1g gravity on ground to +2.5g manoeuvre in flight) on a very flexible aircraft normal modes. The origin of abscissa axis corresponds to the un-deformed or "jig" shape, which is the basis for the A/C design and structure model definition. Broadly speaking, in-flight loads produce a decrease of the normal modes frequency. On the other hand, the on-ground gravity produces a similar effect in some of the modes frequency, but the opposite in others. In other words, the model adjustment to match GVT results might be in the opposite sense to that intended for its applicability to flight.

More information can be found in [7], where it is also shown that the effect of applied loads in a less flexible aircraft is negligible.

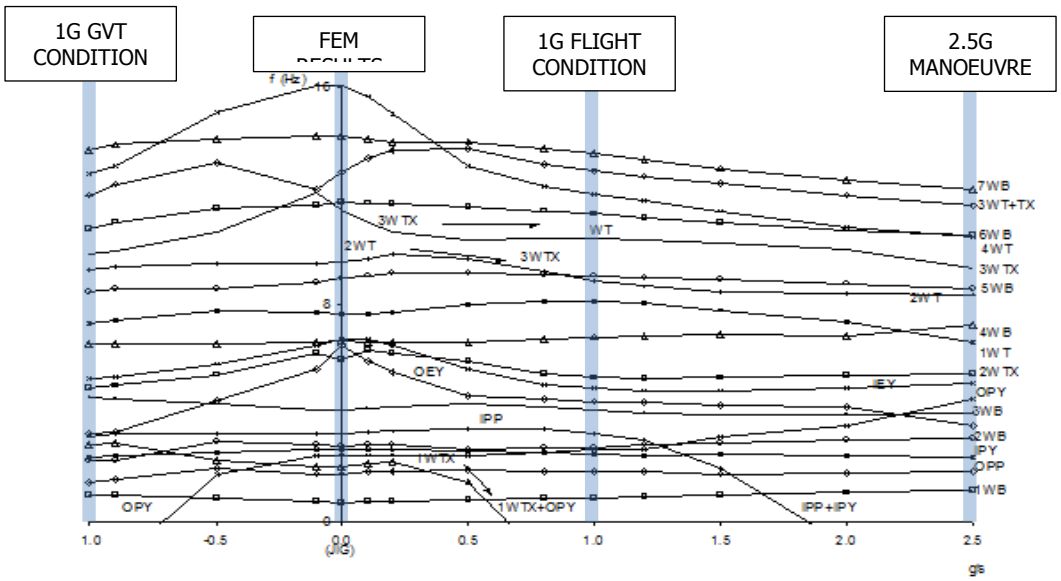

Figure 30: Non-linear effects of applied loads and large deformations on aircraft normal modes

6 CONCLUSIONS

Are normal modes Friends or Foes? … Both?

FOES

- When exciting an aircraft in one of its mode shapes and at the corresponding natural frequency, the amplitudes obtained may be very large with very low level of input excitation. This, in turn, may jeopardize the aircraft structural integrity.
- In presence of unsteady aerodynamics, two or more modes may couple and extract energy from the flow, thus creating the catastrophic instability of **flutter**.
- Modes may be "dangerous companions"; it is the duty of the engineer working in structural dynamics and aeroelasticity to know where they are (frequency) and how they are (mode shape).

FRIENDS

- The dynamic equations expression in the normal modes base allows to reduce the problem size by 3-4 orders of magnitude with almost no lack of accuracy.
- The normal modes of an aircraft may accurately be measured in a Ground Vibration Test, a non-destructive test that can be performed in few weeks producing a fabulous outcome of precious results for the aeroelastician.
- The apparently weird aircraft response to a transient excitation can be better interpreted when illuminated with the light of the aircraft normal modes.

Modes, maybe the aeroelastician best friends…

REFERENCES

[1] A. Tewari; 2015, "Aeroservoelasticity: Modeling and Control"; Birkhäuser.
[2] R.L. Bisplinghoff, H. Ashley, and R.L. Halfmann; 1996; "Aeroelasticity"; Dover.
[3] D.H. Hodges and G.A. Pierce; 2011; "Introduction to Structural Dynamics and Aeroelasticity"; Cambridge University Press.
[4] EASA CS-25; 2007; "Certification Specifications for Large Aeroplanes"; Airworthiness certification; Amendment 3; https://www.easa.europa.eu/system/files/dfu/CS-25_Amdt%203_19.09.07_Consolidated%20version.pdf.
[5] M. Oliver, G. Pastor, M.A. Torralba, S. Claverías, J. Cerezo and H. Climent; 2013; "A400M Aeroelastics and Dynamic Tests". *CEAS 2013 Air and Space Conference*; Linköping, Sweden; 16-20 September.
[6] M. Oliver, J. Rodríguez, J. Martinez, H. Climent, R. de Diego, J. de Alba; 2009; "A400M GVT: The Challenge of Nonlinear Modes in Very Large GVT's". *International Forum of Aeroelasticity and Structural Dynamics IFASD2009*; Seattle, USA; 22-24 June.
[7] M. Oliver, H. Climent and F. Rosich; 1999; "Non-linear Effects of Applied Loads and Large Deformations on Aircraft Normal Modes". *Specialists' Meeting of the RTO Applied Vehicle Technology Panel (AVT)*; Ottawa, Canada; 18-20 October. RTO Meeting Proceedings 36, Chapter 21.